ChemComm

Accepted Manuscript

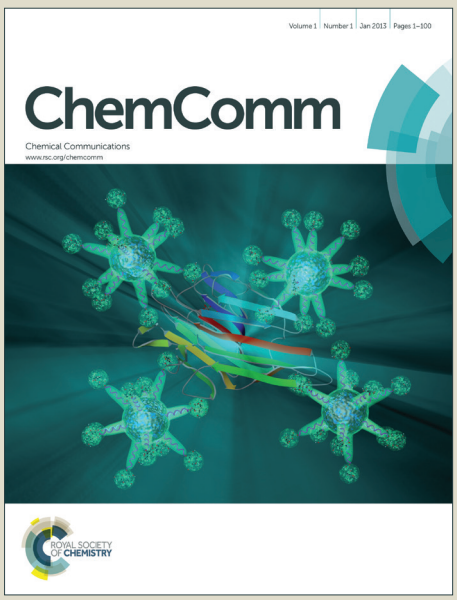

ROYAL SOCIETY OF CHEMISTRY

www.rsc.org/chemcomm

Journal Name

RSCPublishing

COMMUNICATION

New approach to molecular self-assembly through formation of dipeptide-based unique architectures by artificial supersaturation†

Cite this: DOI: 10.1039/x0xx00000x

Received 00th January 2012,
Accepted 00th January 2012

DOI: 10.1039/x0xx00000x

www.rsc.org/

Received (in XXX, XXX) Xth XXXXXXXXX 20XX, Accepted Xth XXXXXXXXX 20XX
DOI: 10.1039/b000000x

Makoto Sakurai,*[a] Pradyot Koley*[a] and Masakazu Aono[a]

Morphological transition and the fabrication of unique architectures through molecular self-assembly of dipeptide is caused by the formation of small nucleus in the artificial supersaturation, achieved by quick drying of the solvent due to the local Joule heating. The growth mechanism of "diatom-like" porous microspheres and microtubes is proposed on the basis of several new techniques developed in the study.

Molecular self-assembly is ubiquitous in nature, and a wide variety of supramolecular nano/micro assemblies with defined morphologies have been constructed through coordinated self-association of biological building blocks including proteins and peptides, by means of various non-covalent interactions.[1-4] In such self-assembled structures, molecular arrangement has been confirmed by X-ray diffraction analysis,[5,6] however, the intermediate growth process to the microstructures has rarely been studied experimentally. Previously reported growth model for the peptide-based microtubes has been proposed solely on the basis of microscopic observation of the final structures.[7-9] Till date there is a substantial gap for the experimental evidence to know preciously about the growth mechanism of biological microstructures. Thus, a deep understanding of the molecular self-assembled process are strongly required for the design and controlled fabrication of biomorphic and biomimetic architectures.

On the contrary, the structural diversity of these peptides assemblies is still limited and there is a great interest in developing new strategies for the construction of intricate morphologies. In the self-assembled complex architectures, the hierarchical cooperation between nano-scale building blocks and the overall micro-scale size plays a key role in the enhancement of the added functionalities of these superstructures.[10-13] However, most of the hierarchical architectures reported to date are created using inorganic materials.[10,14] Fabrication of full-organic specially biomolecule-based architectures has been required to achieve cost-effective and environmental benign applications in catalysis, sensing and cell-cultures.[11-13] The design and controlled fabrication of molecular self-assembled architectures will also lead to great progress in nanomedicines[15] and nanophotonics[16].

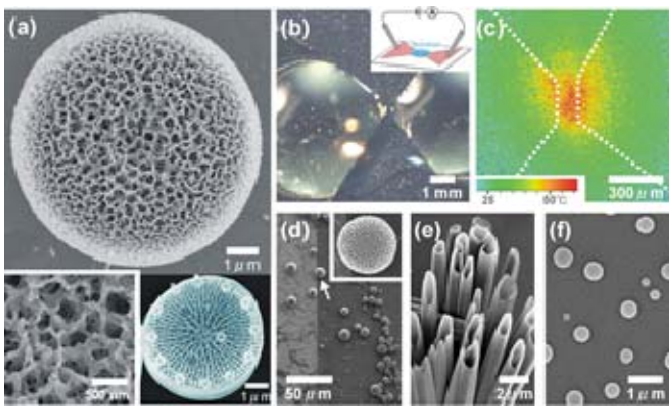

Fig.1 (a) SEM image of porous, "diatom-like" microstructures, and a corresponding higher magnification image showing the surface porosity (left inset); photograph of a microscopic marine diatom (right inset). (b) Configuration of the electrode (inset) and a drop of peptide solution located in the gap between the two Au electrodes. (c) Thermographic map showing the increase of temperature due to Joule heating between the electrodes. SEM images of as-grown (d) porous microspheres and (e) microtubes on the surface of the electrodes. (f) Typical dot-like nanospheres self-assembled from a methanolic solution of FF, without applying voltage.

Here, we show one method of controlled fabrications using a short dipeptide diphenylalanine (FF), which is an important fragment of proteins and has been known as a core recognition motif of Alzheimer's β–amyloid polypeptide.[5,17-19] Self-assembling peptides are very attractive building blocks owing to their chemical diversity, capability of specific molecular recognition, easy availability and functional flexibility.[1-4, 20-21] In this report, the growth of a unique peptide-based flower-like microstructure, which resembles to a marine algae "diatom" in

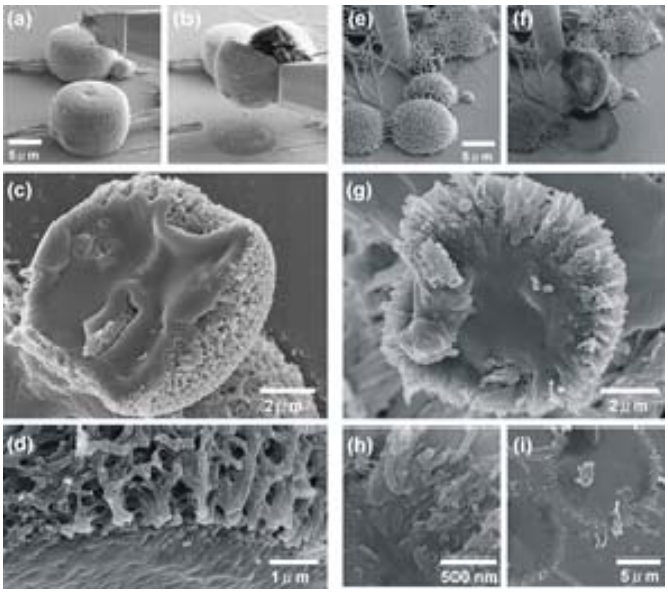

Fig.2 SEM images of (a) before, and (b) after cutting a porous microsphere using a sharp metal probe. Cross-sectional view of (c) the microsphere, showing the smooth amorphous core. (d) Bottom of the microsphere removed using the probe, showing the smooth amorphous surface. SEM images of removal of a microhemisphere from a substrate using a sharp needle (e) before, and (f) after the manipulation. (g) Bottom of a hemisphere also showing the smooth amorphous-like core. (h) Magnified image of interface between the core and the shell. (i) The place from where the hemisphere has been removed and the top right circle corresponds to the place removed in '(f)', which indicates the formation of microtubes below the hemispheres.

shape and size, has been demonstrated through the formation of initial nucleus in presence of artificial supersaturation, that is different from commonly used external stimulus such as solvent polarity, concentration, pH or enzymes to control molecular self-assembly.[4,22-24] We have also studied the intermediate growth process and their growth mechanism by *in situ* monitoring of their real time growth using an optical microscope and by analysis of their internal structures using needle-manipulation combined with scanning electron microscope (SEM).

Figure 1a shows a SEM image of porous microstructures (average diameter 5-10 μm), fabricated using a methanolic solution of diphenylalanine with a concentration of 1 mg/mL. In a typical configuration (inset of Figure 1b), one drop of methanolic solution of FF was placed between two Au electrodes having gap distance of 120 μm (Figure 1b and Movie S1, Supporting Information). Under the application of voltage (e.g., 100 V) between the electrodes, an electric current on the order of 100 μA was observed to pass through the solution (Figure S1, Supporting Information and experimental sections). This caused an increase of temperature in the narrow gap region due to the Joule heating effect (Figure 1c). After drying of the solvent (3-6 min.), several porous microspheres and microtubes were observed on the substrate **(**Figures 1d and e). The microsphere closely resembles to a microscopic marine algae diatom (lower inset of Figure 1a). The high-magnification SEM image reveals the surface morphology of the microsphere, where wires (average diameter 50-100 nm) with many protrusions are tangled together in three-dimensional network structures (upper inset of Figure 1a), which are quite similar to the frustule of diatoms. Under the application of a typical voltage of 100 V, the initial growth stage in the formation of the microstructures requires the applying time of approximately 25-30 s, after the dropping of 4 μL solution. As the methanolic solutions of FF typically self-assemble to form spherical, dot-like structures with diameters of 100-400 nm (Figure 1f)[25]; our results showed a clear-cut morphological transition from nanoscale dot-like structures to microscale spheres and tubes. The structural integrity of the FF molecules in the porous microspheres and microtubes was confirmed using time-of-flight secondary ion mass spectroscopy (TOF-SIMS) (Figure S2).[18]

To confirm the influence of temperature, electric field, and electric current in the formation of the microstructures, we performed several systematic experiments. Three different types of electrode pattern were prepared in which the same order of electric field (10^5-10^7 V/m) was maintained, but without any current flowing (Figure S3). These electrodes configurations failed to produce any novel microstructures; rather, the typical dot-like spheres were observed similar to without applying voltage. Moreover, uniform increase of the bulk solution temperature (30–70°C) up to the boiling temperature of methanol using a heater also failed to produce any microstructures. These results helped us to exclude the possibility of electric field and bulk temperature from the list of potential factors influencing the formation of the microstructures. The temperature distribution shown in Figure 1c also indicates a wide current-flow path between the electrodes; we could therefore neglect the influence of the current, because of the low current density (~1×10^{-10} A/μm^2) in this configuration. The formation of porous microstructures by a different type of artificial supersaturation caused by a Joule heating of narrow metal wires between the electrodes with low applied voltage of 0.5 V, excludes the possibility of any electrochemical reaction for their formation (Figure S4).

We used needle-manipulation under SEM observation to study the internal morphology of the porous microspheres. Figure 2a and b shows the SEM images taken before and after the cutting operation using a sharp "knife-like" needle, respectively. The cross-sectional view of the microsphere clearly shows that the morphology of the core materials is completely different from that of the shell structures (Figure 2c). The average shell thickness (measured from different microspheres) is in the range of 0.5 - 1.0 μm. Figure 2b also indicates the place from where the microsphere was removed, and this place is lower than the surrounding area. At the time of cutting operation, it was observed that the core of the microsphere was soft enough (Movie S2). Figure 2d depicts magnifid image of the bottom of the microsphere, removed from the substrate by the needle.

The cutting operation usually deformed the microspheres, then we performed the removal of the microstructures using a

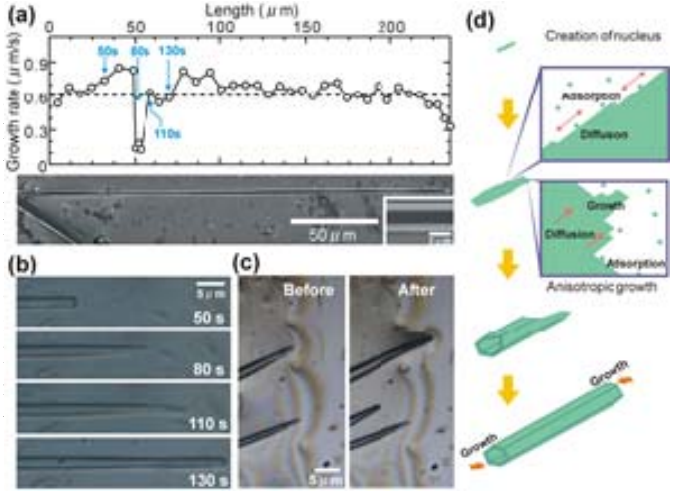

Fig.3 (a) Plot of growth rate vs. time at each position for a typical microtube, and the corresponding SEM image. Optical microscopy images showing (b) the shape of the apex of the microtube at each time point, and (c) the end portion of the tube growing and approaching the boundary. (d) Schematic illustration of the growth from a regularly arranged nucleus to a microtube

growth of the FF microtubes to understand their growth mechanism in detail. Figure 3a shows the growth rate at each position for a typical microtube (SEM image in Figure 3a). The average growth rate of the tube is ~ 0.6 μm/s. After 80 s of growth, the growth rate reduced to 0.15 μm/s, but the growth rate had returned to the average value after 110 s. The optical microscope images in Figure 3b depict the apex of the microtube at each growth time, corresponding to the points shown in Figure 3a. The apex of the tube shows an almost flat shape under the constant growth rate (0.6 μm/s), but under the slower growth rate (0.15 μm/s), the shape of the apex becomes sharp and narrower (Figure 3b). These temporal changes in the shape suggest that a shortage in the supply of molecules near the apex of the tube leads to the decrease in the growth rate and the imperfect shape (Movie S3). After 30 s of the slow rate, it recovers to the average value, and the apex also regains to its original flat shape (Figure 3b). This phenomenon indicates the self-healing nature of the FF microtube growth; this is also supported by the uniform diameter of the microtube observed in the SEM image (bottom of Figure 3a). The almost constant growth rate shown in Figure 3a suggests that there is a balance between supply and growth in the solution. Figure 3c shows the optical microscope images of microtubes growth near the boundary of the solution (Movie S4). The end portion of the tube grows elongated to the boundary ('Before' in Figure 3c), and pushing the edge leads to the expansion of the boundary ('After' in Figure 3c). If we assume that the molecules are supplied by direct adsorption on the growing apex, the situation shown in Figure 3c cannot be explained, because there is no molecule-supplying source near the boundary. It is therefore likely that the molecules at the growing apex are provided mainly via the diffusion of molecules along the surface of the tubes. The shape of the tube indicates to the anisotropic diffusion; the molecules on the surface prefer to diffuse in the direction parallel to the tube.

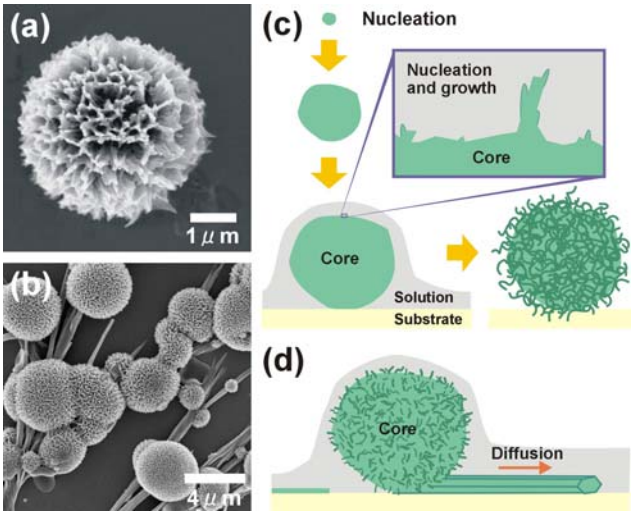

Fig. 4 **SEM images of (a) smaller microspheres, and (b) the coexistence of microtubes and "diatom-like" microspheres on a substrate, where the microspheres grow just above the microtubes. Schematic illustration showing (c) the growth from a randomly arranged nucleus to a porous microsphere, and (d) the diffusion of residual adsorbents along the flat and smooth surface of the microtubes.**

Figure 4a shows a SEM image of comparatively smaller "diatom-like" porous microspheres and Figure 4b demonstrates the coexistence of microtubes and microspheres on the substrate, where the microspheres are grown just above the microtubes. It was also observed in SEM images taken after the needle manipulation (Figure 2i). In addition, note that the porosity of the structures are formed only on the surface of the microspheres, not on the microtubes, as shown in Figure 4b; whereas organic layers stacked on the substrate do not produce any structures (Figures 2b and f). The growth rate of the microspheres, which is defined as a change of the diameter per unit time, is about 1–2 order magnitude slower than that of the microtubes.

The results for the formation of two different microstructures can't be explained by the previous model based on merging of nanostructures.[7-9] The growth mechanism of these microstructures is similar to that of a simple crystal growth,[26] which consists of three steps: nucleation, adsorption and diffusion, and growth. Self-assembled microstructures have the similar packing arrangements in their nucleation stage, suggesting the formation of two different initial nuclei in the solution. The nuclei are formed because of the supersaturation caused by the drying of solvents due to a Joule heating effect as shown in Figure 1c and in the visible bubbling of the solution (Movie S1). The supersaturation and the larger molecular mobility due to the increase in the temperature promote aggregation of the molecules.

At the place slightly far from the gap region where the evaporation takes places, regularly arranged nuclei are created thermodynamically because of low concentration of the small aggregations. As illustrated schematically in Figure 3d, the large arranged aggregate, which has a flat and smooth surface,

acts as a nucleus for the growth of microtubes. The diffusion of molecules along the surface leads to a supply of the molecules at the apex of the structure and facilitate the formation of a microtube. The microtube has a hexagonal cross section (Figure 1e and inset of Figure 3a), because FF dipeptide molecules have an inherent tendency to arrange regularly in a hexagonal packing pattern under the influence of their mutual noncovalent interactions.[5,8] Whereas, at the gap region or near to the gap region, the number density of small aggregated molecules is relatively high. Their mutual collision and adsorption leads to the formation of large amorphous-like aggregates acting as nucleus (Figure 4c). The surfaces of these nuclei are not flat and smooth. So, the molecules adsorbing on the surface cannot diffuse on it. The amorphous-like core therefore grows uniformly and spherically, as shown in Figure 2. In the final stage of drying, another supersaturation event takes places, because drying of the solvent from the surface of the residual solution occurs near the growth position. The high concentration causes creation and merging of small aggregations on rough surfaces of the microspheres, leading to the formation of the porous shell. In contrast, in the case of the microtubes, the adsorbents from the residual solution diffuse along the flat and smooth surface to the apex of the tube, as shown schematically in Figure 4d. The rough surface of the microspheres in laser scanning microscope image (Figure S7) supports the formation of shell.

The present fabrication method was also applied to an analogous short dipeptide phenylalanine-tyrosine (FY), where one of the phenylalanine residues has been replaced by tyrosine. Morphological transition and the formation of flower-like microstructures of the peptide under similar experimental conditions, clearly indicates towards the generality of the present method for the controlled fabrication of hierarchical self-assembled architectures from short peptides (Figure S8).

Conclusions

In this study, we have demonstrated a simple preparative method and the precise growth mechanism for the production of "diatom-like" complex architectures from a simple dipeptide. Morphological transition and the fabrication of unique microstructures in the molecular self-assembly are caused by the formation of tiny nucleus induced by the artificial supersaturation for the first time. The microspheres have the similar porous structure to that of diatom, whose structures have been known as sensitive biosensors.[27,28] Therefore, the replacement of the short peptide to other functional biomolecules such as fluorescent proteins, polypeptides or enzymes as well as some modification of the dipeptide with a chromophore or fluorophore may also produce hierarchical functional biomaterials, which will achieve cost-effective and environmental friendly biosensors, biophotonic devices and biocatalysts. Moreover, the unique analytic methods will also lead to a deep understanding of the molecular self-assembly, which will pave the way for the development and discovery of new biomorphic and biomimetic materials from different biomolecules.

This work was supported in part by the World Premier International Center (WPI) Initiative on Materials Nanoarchitectonics, MEXT, Japan. We thank Dr. Shimomura, Dr. Miyazawa, Dr. Miyazaki, Dr. Kasaya of NIMS for the needle-manipulation, Dr. H. Iwai of NIMS for the operation of TOF-SIMS, and Prof. T. Ueta of the Jikei University School of Medicine for discussion about growth mechanism, and Prof. C. Joachim of CNRS and NIMS and Dr. Y. Okawa of NIMS for useful comments and discussion.

Notes and references

[a] *International Center for Materials Nanoarchitectonics (WPI-MANA), National Institute for Materials Science (NIMS), 1-1 Namiki, Thukuba, 305-0044, Japan. Fax: +81-29-860-4890; Tel: +81-29-859-2000; E-mail: sakurai.makoto@nims.go.jp (SK); pradyot.koley@gmail.com (PK)*

† Electronic Supplementary Information (ESI) available: Materials and methods, supplimentary text, Fig. S1-S8 and movie S1-S4. See DOI: 10.1039/b000000x/

1 G. M. Whitesides, J. P. Mathias and C. T. Seto, *Science,* 1991, **254**, 1312.
2 E. Gazit, *Nature Chem*., 2010, **2**, 1010.
3 S. Zhang, *Nature biotechnology*, 2003, **21**, 1171.
4 R. J. Williams, A. M. Smith, R. Collins, N. Hodson, A. K. Das and R. V. Ulijn, *Nature Nanotech*., 2009, **4**, 19.
5 C. H. Görbitz, *Chem. Commun.*, 2006, 2332.
6 C. H. Görbitz, *Chem. Euro. J*., 2007, **13**, 1022.
7 M. Wang, L. Du, X. Wu, S. Xiong and P. K. Chu, *ACS Nano,* 2011, **5**, 4448.
8 X. Yan, H. Möhwald and J. Li, *Adv. Mater*., 2011, **23**, 2796.
9 W. Wang and Y. Chau, *Soft Matter,* 2009, **5**, 4893.
10 J. Ge, J. Lei and R. N. Zare, *Nature Nanotechnol*., 2012, **7**, 428.
11 S. Kiyonaka, K. Sada, I. Yoshimura, S. Shinkai, N. Kato and I. Hamachi, *Nature Mater*., 2004, **3**, 58.
12 Y. Cui, S. N. Kim, R. R. Naik and M. C. Mcalpine, *Acc. Chem. Res*., 2012, **45**, 696.
13 G. A. Silva, C. Czeisler, K. L. Niece, E. Beniash, D. A. Harrington, J. A. Kessler and S. I. Stupp, *Science,* 2004, **303**, 1352.
14 W. L. Noorduin, A. Grinthal, L. Mahadevan and J. Aizenberg, *Science,* 2013, **340**, 832.
15 M. J. Webber, J. A. Kessler and S. I. Stupp, *J. Inter. Med*., 2009, **267**, 71.
16 C. M. Drain, *Proc. Natl. Acad. Sci. USA,* 2002, **99**, 5178.
17 M. Reches and E. Gazit, *Science,* 2003, **300**, 625.
18 L. Adler-Abramovich, D. Aronov, P. Beker, M. Yevnin, S. Stempler, L. Buzhansky, G. Rosenman and E. Gazit, *Nature Nanotech*., 2009, **4**, 849.
19 X. Yan, P. Zhu and J. Li, *Chem. Soc. Rev.,* 2010, **39**, 1877.
20 S. Vauthe, S. Santoso, H. Gong, N. Watson and S. Zhang, *Proc. Natl. Acad. Sci. USA*, 2002, **16**, 5355.
21 K. H. Smith, E. T. -Montes, M. Poch and A. Mata, *Chem. Soc. Rev*., 2011, **40**, 4563.
22 T. O. Mason, D. Y. Chirgadze, A. Levin, L. A. Abramovich, E. Gazit, T. P. J. Knowles and A. K. Buell, *ACS Nano,* 2014, **8**, 1243.
23 R. V. Uijin and A. M. Smith, *Chem. Soc. Rev.,* 2008, **37**, 664.
24 P. Koley and A. Pramanik, *Adv. Funct. Mater*., 2011, **21**, 4126.
25 N. Amdursky, M. Molotskii, E. Gazit and G. Rosenman, *J. Am. Chem. Soc*., 2010, **132,** 15632.
26 Y. Saito, Statistical Physics of Crystal Growth (World Scientific, Singapore, 1996).
27 A. Scheffela, N. Poulsena, S. Shianb and N. Kröger, *Proc. Natl. Acad. Sci. USA*, 2011, **108**, 3175.
28 K. E. Marshall, E. W. Robinson, S. M. Hengel, L. Paša.-Tolić and G. FRET Roesijadi, *PLoS ONE,* 2012, **7**, e33771

